Strong mobility degradation in ideal graphene nanoribbons due to phonon scattering

A. Betti,[a] G. Fiori, and G. Iannaccone
Dipartimento di Ingegneria dell'Informazione: Elettronica, Informatica, Telecomunicazioni, Università di Pisa, Via Caruso 16, I-56122 Pisa, Italy

(Received 27 January 2011; accepted 15 April 2011; published online 27 May 2011)

We investigate the low-field phonon-limited mobility in armchair graphene nanoribbons (GNRs) using full-band electron and phonon dispersion relations. We show that lateral confinement suppresses the intrinsic mobility of GNRs to values typical of common bulk semiconductors, and very far from the impressive experiments on two-dimensional graphene. 1 nm-wide suspended GNRs exhibit a mobility close to 500 $cm^2/V\,s$ at room temperature, whereas 1 nm-wide GNRs deposited on HfO_2 exhibit a mobility of 60 $cm^2/V\,s$ due to surface phonons. We also show the occurrence of polaron formation, leading to band gap renormalization of ≈118 meV for 1-nm-wide armchair GNRs. © *2011 American Institute of Physics*. [doi:10.1063/1.3587627]

Understanding the role of phonon scattering[1–3] is of primary importance, since it provides information regarding the ultimate *intrinsic* mobility limit (μ_{in}) of a material, i.e., when all *extrinsic* scattering sources have been removed. This is especially important for new materials or nanostructured ones, such as graphene nanoribbons (GNRs), where experiments are not fully comparable, given the presence of defects and other non idealities. Recent experiments have found μ_{in} in suspended graphene close to 10^5 $cm^2/V\,s$ near room temperature (RT),[4] but with a sizable degradation after deposition on high-k gate insulators,[5] probably due to coupling to the polar modes of the substrate.[1,2]Very few indications are available on mobility degradation in GNRs deposited on different gate insulators.[6] As of now, μ_{in} in sub-10 nm GNRs cannot be extracted from experiments since line-edge roughness (LER) is presently limiting mobility in state-of-the-art GNRs.[7,8] Theory, on the other hand, allows us to individually evaluate the impact of each scattering source on mobility, which is often a prohibitive task in experiments.

Here we investigate the effect of phonons and surface optical (SO) phonons on carrier transport in GNRs by means of a full band (FB) approach based on a tight-binding (TB) description[9] of the electronic structure and of the phonon spectrum. We compute scattering rates with first-order perturbation theory using the deformation potential approximation (DPA), and low-field mobility using the Kubo–Greenwood formula.[10] We obtain the one-dimensional (1D) subbands of an armchair GNR from a TB p_z-Hamiltonian accounting for energy relaxation at the edges.[11] The electron energy dispersion is quantized in the transverse direction y with wavevectors $k_{y\eta}=(2\pi\eta)/[(l+1)a]$, where $a=0.249$ nm is the graphene lattice constant, l is the number of dimer lines and index η runs from 1 to l. Graphene phonon spectrum is obtained with the force constant dynamic-matrix approach, including contributions up to the fourth nearest neighbors (4NNFC approach)[9] and using force constant parameters extracted from first-principles calculations.[12] Each of the six phonon branches of graphene, labeled by the quantum number j, is split into l 1D subbranches, with transverse wave vector $q_{y\beta}$ $(\beta=0,\ldots,l-1)$.[10] The momentum relaxation rate of an electron in the initial state $\mathbf{k}=(k_x,k_{y\eta})$ accounting for scattering from GNR phonons is obtained from the Fermi golden rule, summing over all final states $\mathbf{k}'=(k'_x,k_{y\eta'})$, conserving total energy and longitudinal momentum:[10]

$$\frac{1}{\tau(\mathbf{k})}=\sum_{\eta'=1}^{l}\sum_{j=1}^{6}\sum_{\beta}\int_{-k_F}^{+k_F}dq_x\frac{n_{\mathbf{q}}^{\mp}\hbar D_j^2}{4\rho W E_{ph}^{j\beta}}(1+\cos\theta_{\mathbf{kk}'})(1-k'_x/k_x)\,G_{\eta,\eta',\beta}\delta[E(\mathbf{k}')-E(\mathbf{k})\mp E_{ph}^{j\beta}(\mathbf{q})]f_{\mathbf{k}'\mathbf{k}},\tag{1}$$

where $D_j=qD_{\mathrm{AC}}$ $(D_j=D_{\mathrm{OP}})$, if j is a longitudinal acoustic (in-plane optical) mode, D_{AC} and $D_{\mathrm{OP}}=1.4\times10^{11}$ eV/m (Ref. 3) are the acoustic (AC) and optical (OP) deformation potentials, respectively, $k'_x=k_x\pm q_x$, $q=|\mathbf{q}|=(q_x^2+q_{y\beta}^2)^{1/2}$, $\rho\approx7.6\times10^{-8}$ g/cm^2 is graphene mass per unit area,[3] $n_{\mathbf{q}}^-$ is the Bose–Einstein occupation factor and $n_{\mathbf{q}}^+=n_{\mathbf{q}}^-+1$. In addition, $k_F=\pi/(\sqrt{3}a)$, $W=a/2(l-1)$ is the GNR width, $(1+\cos\theta_{\mathbf{kk}'})$ is the spinor overlap, $f_{\mathbf{k}'\mathbf{k}}=[1-f(E_{\mathbf{k}'})]/[1-f(E_{\mathbf{k}})]$ is the degeneracy factor and $f(E)$ is the Fermi occupation factor. In Eq. (1) the upper sign is for phonon absorption and the lower for phonon emission. $G_{\eta,\eta',\beta}$ is the form factor due to the transverse momentum conservation uncertainty (TMCU).[10,13]

We have investigated the electrostatic coupling between electrons in the GNR channel and remote phonons of the substrate considering the GNR deposited on an oxide layer of thickness t_{ox}, width W_{ox} and placed at a distance $d=0.4$ nm, neglecting any modifications of GNR band structure.[14]In addition, since remote phonon modes are almost constant as a function of the longitudinal SO phonon wavevector,[2] we assume the same energies E_{SO}^{β} as in Ref. 1 for the two considered SO phonon modes. Since electrons are confined in the plane, the electron-SO phonon scattering rate reads:[10]

$$\frac{1}{\tau(\mathbf{k})}=\sum_{\eta'=1}^{l}\sum_{\beta}\int d\mathbf{Q}\frac{LW_{ox}e^2F_{\beta}^2Ge^{-2Qd}}{4\pi\hbar[\epsilon_{1\mathrm{D}}(Q_x)]^2Q}(1+\cos\theta_{\mathbf{kk}'})n_{\mathbf{Q}}^{\mp}\delta(E_{\mathbf{k}'}-E_{\mathbf{k}}\mp E_{\mathrm{SO}}^{\beta})(1-k'_x/k_x)f_{\mathbf{k}'\mathbf{k}},\tag{2}$$

where $\mathbf{Q}=(Q_x,Q_y)$ represents the two-dimensional (2D) SO

[a]Electronic mail: alessandro.betti@iet.unipi.it.

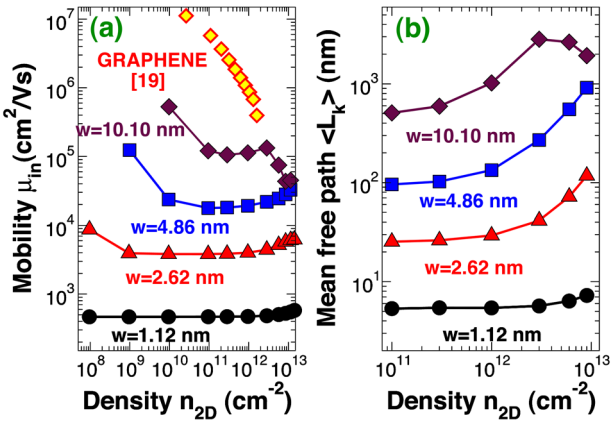

FIG. 1. (Color online) (a) μ_{in} and (b) $\langle L_{\mathbf{k}}\rangle$ for an electron in the lowest subband as a function of n_{2D} for different W. DFT calculations (Ref. 19) for graphene are also shown in (a).

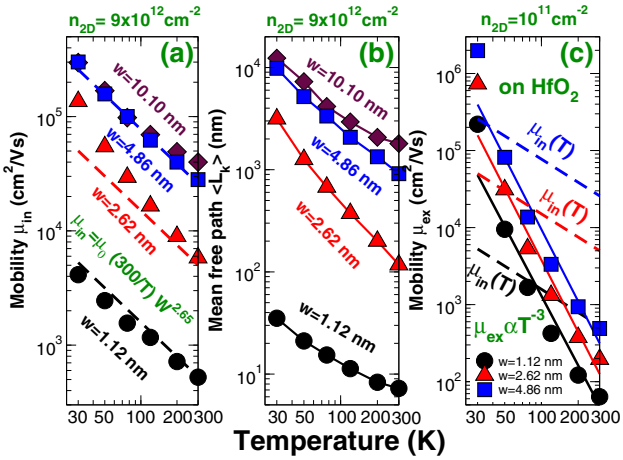

FIG. 2. (Color online) (a) Mobility μ_{in}, (b) mean free path $\langle L_{\mathbf{k}}\rangle$ for the lowest subband, and (c) mobility μ_{ex} for GNR on HfO_2 as a function of T for different W. In (a) and (c) dashed lines correspond to the empirical formula for $\mu_{in}(W,T)$ and solid lines in (c) to the fit for μ_{ex}.

phonon wavevector, $Q=|\mathbf{Q}|$, the sum Σ_β runs over all SO phonon modes, $F_\beta^2 \propto 1/(LW_{ox})$ is the electron-phonon coupling parameter[2,10] and $G(\eta,\eta',Q_y)$ is the form factor[10] which reduces to $G_{\eta,\eta',\beta}$ if $Q_y=q_{y\beta}$.

In Eq. (2), $\epsilon_{1D}(Q_x)$ is the GNR static dielectric function calculated within the random phase approximation (RPA) in the size quantum limit.[3,10] For 10-nm-wide GNRs, screening is instead modeled by means of the 2D RPA graphene static dielectric function $\epsilon_{2D}(Q)$.[15] From a numerical point of view, we have approximated δ in Eqs. (1) and (2) with a Gaussian window of standard deviation ΔE and, for the lowest AC subbranches, a collisional broadening approach has been implemented considering $\Delta E=\hbar/2[1/\tau(\mathbf{k},q_{y\beta})]$. Finally, we have computed the low-field mobility μ_{in} by means of the Kubo–Greenwood formula.[10,13]

DPA formally leads to a zero coupling with the transversal acoustic (TA) and flexural (ZA) phonon modes, so that only scattering with longitudinal acoustic (LA) modes is typically considered.[3] Theory[16] and Raman spectroscopy[17] have shown that ZA modes are negligible down to 130 K. However, classical results based on a TB description of electron-phonon coupling[18] and recent *ab initio* calculations[19] have demonstrated that TA modes play a comparable role as that of LA modes in degrading μ_{in}. On the other hand, by taking into account long-range interaction between carbon atoms,the off-diagonal coupling to the TA modes, through the modulation of the hopping parameters, is smaller than the on-diagonal deformation potential contribution.[20] We choose to adopt DPA considering electron coupling only with LA, LO, and TO modes, rather than heuristically reintroduce the contribution of TA modes. We use $D_{AC}=10.9$ eV, extracted from density functional theory (DFT) calculation for the GNR family $3l+1$,[21] rather than fitting experiments which actually lead to a large spread of the considered values for D_{AC}.[3,4,19]

Low-field mobility is shown in Fig. 1(a) as a function of the electron density n_{2D} for different widths. μ_{in} close to 500 $cm^2/V\,s$ is found for 1-nm-wide GNR, exceeding by almost one order of magnitude the experimental mobility of GNRs (Ref. 7) and μ_{in} of silicon nanowires (SNWs)[22] of comparable size. We find that μ_{in} is mainly limited by backward scattering involving AC phonons, due to the large mode-dependent OP energy offset (≈130–160 meV).[13] Unlike in 2D graphene, where $\mu_{in}\propto 1/n_{2D}$,[1] the lateral confinement in GNRs leads to a nonmonotonic n_{2D}-dependence as also observed in carbon nanotubes (CNTs) (Ref. 23) [Fig. 1(a)]. For small W, μ_{in} increases with n_{2D}, due to the reduction in final states available for scattering. For wider GNRs biased in the inversion regime, electrons can populate excited subbands opening additional channels for scattering, thus reducing μ_{in}.

In Fig. 2(a), μ_{in} is plotted as a function of temperature T. Similarly to what has been observed in small-diameter CNTs,[24] in narrow GNRs the dependence on W and T can be expressed by means of the empirical relation $\mu_{in}(W,T)=\mu_0(300\ \mathrm{K}/T)(W/1\ \mathrm{nm})^{\alpha_{AC}}$ where $\mu_0\approx 391\ cm^2/V\,s$ and $\alpha_{AC}=2.65$, which is close to $\mu_{in}\propto W^3$ expected for narrow GNRs, since $\mu_{in}\propto\tau/(W\times \mathrm{DOS})\propto G^{-1}\mathrm{DOS}^{-2}$ and $G\propto 1/W^2$ and the density of states $\mathrm{DOS}\propto 1/\sqrt{W}$. Of course, for large W μ_{in} saturates to that of 2D graphene. Since AC in-plane phonons scattering is dominant and $n_{\mathbf{q}}^-\approx kT/\hbar\omega$ for $kT\gg\hbar\omega$, $\mu_{in}\propto 1/T$ [Fig. 2(a)]. The mean free path in the first subband $\langle L_{\mathbf{k}}\rangle$ is shown in Fig. 1(b) as a function of n_{2D} and in Fig. 2(b) as a function of T, where $\langle L_{\mathbf{k}}\rangle\equiv\langle v(\mathbf{k})\tau(\mathbf{k})\rangle$, $v(\mathbf{k})$ is the group velocity and the expectation value $\langle\cdot\rangle$ has been computed in the Brillouin zone, considering $f(1-f)$ as the distribution function.[13] At $T=300$ K, $\langle L_{\mathbf{k}}\rangle$ is of the order of few micrometer for larger GNRs, as expected in graphene flakes, while it is ≈10 nm for narrower GNRs [Fig. 2(b)]. In addition, $\langle L_{\mathbf{k}}\rangle\propto 1/T$, as μ_{in}.

The SO phonon-limited mobility μ_{ex} as a function of n_{2D} is shown in Figs. 3(a) and 3(b) for W smaller than 10 nm, considering GNRs deposited both on SiO_2 and on HfO_2. As in graphene,[1,2] the higher the dielectric constant, the larger the mobility suppression due to SO phonon scattering. In particular, we observe μ_{ex} down to 700 $cm^2/V\,s$ for SiO_2 [Fig. 3(a)] and 60 $cm^2/V\,s$ for HfO_2 [Fig. 3(b)], due to the smaller energy offset of the EM processes. As in CNTs,[25] $\mu_{ex}\propto W^{\alpha_{SO}}$ with α_{SO} (≈1.4–1.6) dependent on n_{2D} and smaller than α_{AC}. For $W<5$ nm μ_{ex} increases with n_{2D} due to the impact of screening, whereas for $W=10.10$ nm for higher concentrations n_{2D} the increase in available modes for scattering reduces mobility. Comparing Figs. 3(a) and 3(b) with Fig. 1(a), it can be observed that SO phonons play a secondary role for very narrow GNRs on SiO_2 but they become predominant with increasing $W\geq 2.5$ nm roughly for

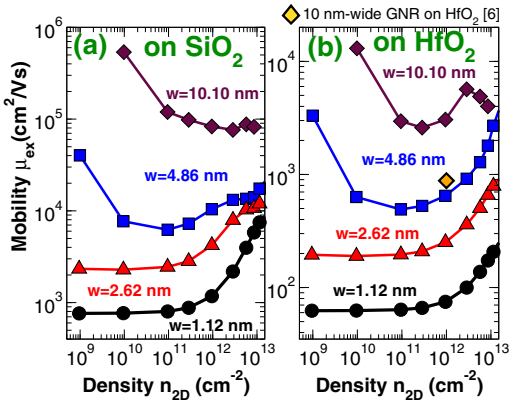

FIG. 3. (Color online) μ_{ex} as a function of n_{2D} for GNR deposited (a) on SiO_2 and (b) on HfO_2.

$n_{2D} < 10^{12}$ cm^{-2}, whereas they are predominant for all n_{2D} densities in GNRs on HfO_2. Comparison with experiments shows that μ_{ex} is larger by up to one order of magnitude than mobility measured on GNRs deposited on SiO_2 (Ref. 7) and by a factor three than mobility measured on 10-nm-wide GNRs integrated with ultrathin HfO_2 dielectric.[6] This gives a rough estimation of the increase in mobility that could be achieved through fabrication technology improvements. As can be noted in Fig. 2(c) and as it also occurs in CNTs deposited on polar dielectrics,[25] $\mu_{ex} \propto 1/T^{\gamma}$. In particular, for HfO_2 $\gamma \approx 3$. Since $\mu_{in} \propto 1/T$, SO phonon scattering dominates transport roughly above 100 K for all W [Fig. 2(c)], as for CNTs on SiO_2.[25]

Finally, we focus on the polaronic energy shift $\delta E_{\mathbf{k}}$ due to the electron-phonon coupling, computed exploiting the second-order perturbation theory.[10] Figure 4(a) shows $\delta E_{\mathbf{k}}$ as a function of $E_{\mathbf{k}}$ for the lowest two subbands for the $W = 1.12$ nm case. $\delta E_{\mathbf{k}}$ is weakly energy dependent near the cutoff subband, is independent of T and increases sharply in correspondence of intersubband transitions. As in CNTs,[24] mostly OP phonons contribute to $\delta E_{\mathbf{k}}$ [inset of Fig. 4(a)]. Instead, unlike in CNTs,[24] the contribution to $\delta E_{\mathbf{k}}$ from AC phonons exhibits few peaks due to TMCU [inset of Fig. 4(a)]. The polaronic binding energy is $\delta E_b = \delta E_{\mathbf{k}}(E_{\mathbf{k}} = E_{C1})$, where E_{C1} is the first subband edge, is almost 59 meV for 1-nm-wide GNRs, close to that obtained for semiconducting CNTs with the same number l (Ref. 24) [Fig. 4(b)] and corresponds to a band gap renormalization $2\delta E_b \approx 118$ meV for 1 nm GNRs, and to a relative correction of -35% of the energy gap E_g of 10 nm nanoribbons [Fig. 4(b)].

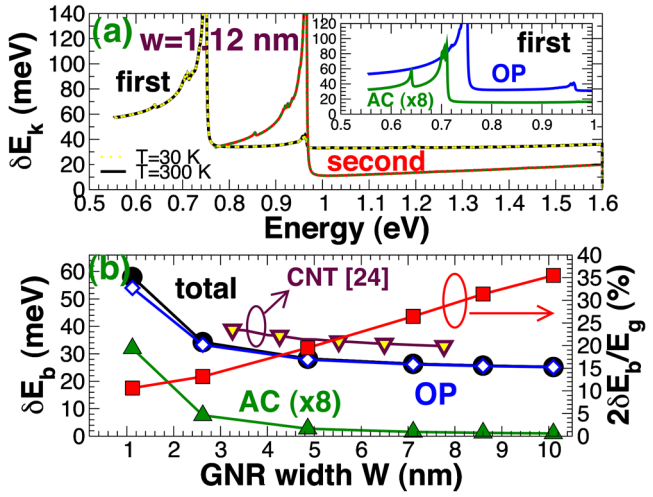

FIG. 4. (Color online) (a) Polaronic energy shift $\delta E_{\mathbf{k}}$ as a function of the energy $E_{\mathbf{k}}$ for the first two subbands ($W = 1.12$ nm). Solid curves correspond to $T = 300$ K, dotted curves to $T = 30$ K. Inset: OP and AC ($\times 8$) contributions to $\delta E_{\mathbf{k}}$ for the first subband. (b) Polaronic binding energy δE_b (left) and polaronic correction to the band gap $2\delta E_b/E_g$ (right) as a function of W. Results for CNTs (Ref. 24) are also reported.

In conclusion, we have proposed a very accurate FB approach to evaluate μ_{in} in GNRs. We find that μ_{in} is close to 500 $cm^2/V\,s$ in suspended 1-nm-wide GNRs at room temperature, and is suppressed down to 60 $cm^2/V\,s$ in 1-nm-wide GNR deposited on HfO_2, due to coupling with SO phonons. The result is important from the point of view of methodology and of fundamental physics, since $\langle L_{\mathbf{k}} \rangle$ ranges from 1 to 10 nm, undermining the possibility of performing ballistic or coherent transport experiments at non-cryogenic temperatures. In addition, narrow GNRs with reasonable semiconducting gap have only slightly larger mobility than comparable SNWs. Finally, we also find polaron formation in armchair GNRs, with a remarkable band gap renormalization of up to 35% for $W = 10$ nm.

This work was supported in part by the EC 7FP through NANOSIL (Grant No. 216171), GRAND (Grant No. 215752) grants, and by the MIUR-PRIN project GRANFET (Prot. 2008S2CLJ9). Authors thank www.nanohub.org.

[1] V. Perebeinos and P. Avouris, Phys. Rev. B **81**, 195442 (2010).
[2] A. Konar, T. Fang, and D. Jena, Phys. Rev. B **82**, 115452 (2010).
[3] T. Fang, A. Konar, H. Xing, and D. Jena, Phys. Rev. B **78**, 205403 (2008).
[4] K. I. Bolotin, K. J. Sikes, J. Hone, H. L. Stormer, and P. Kim, Phys. Rev. Lett. **101**, 096802 (2008).
[5] J.-H. Chen, C. Jang, S. Xiao, M. Ishigami, and M. S. Fuhrer, Nat. Nanotechnol. **3**, 206 (2008).
[6] L. Liao, J. Bai, R. Cheng, Y.-C. Lin, S. Jiang, Y. Huang, and X. Duan, Nano Lett. **10**, 1917 (2010).
[7] X. Wang, Y. Ouyang, X. Li, H. Wang, J. Guo, and H. Dai, Phys. Rev. Lett. **100**, 206803 (2008).
[8] A. Betti, G. Fiori, and G. Iannaccone, IEEE Trans. Electron Devices (to be published).
[9] R. Saito, G. Dresselhaus, and M. Dresselhaus, *Physical Properties of Carbon Nanotubes* (Imperial College Press, London (2003).
[10] See supplementary material at http://dx.doi.org/10.1063/1.3587627 for the expressions of $q_{y\beta}$, $1/\tau(\mathbf{k})$, μ, and $\delta E_{\mathbf{k}}$.
[11] Y. W. Son, M. L. Cohen, and S. Louie, Phys. Rev. Lett. **97**, 216803 (2006).
[12] L. Wirtz and A. Rubio, Solid State Commun. **131**, 141 (2004).
[13] A. Betti, G. Fiori, and G. Iannaccone, Tech. Dig. - Int. Electron Devices Meet. **2010**, 728.
[14] Y. Wang, Z. Ni, T. Yu, Z. Shen, H. Wang, Y. Wu, W. Chen, and A. Wee, J. Phys. Chem. C **112**, 10637 (2008).
[15] E. H. Hwang, S. Adam, and S. D. Sarma, Phys. Rev. Lett. **98**, 186806 (2007).
[16] E. Mariani and F. von Oppen, Phys. Rev. Lett. **100**, 076801 (2008).
[17] A. C. Ferrari, J. C. Meyer, V. Scardaci, C. Casiraghi, M. Lazzeri, F. Mauri, S. Piscanec, D. Jiang, K. S. Novoselov, S. Roth, and A. K. Geim, Phys. Rev. Lett. **97**, 187401 (2006).
[18] L. Pietronero, S. Strässler, and H. R. Zeller, Phys. Rev. B **22**, 904 (1980).
[19] K. M. Borysenko, J. T. Mullen, E. A. Barry, S. Paul, Y. G. Semenov, J. M. Zavada, M. B. Nardelli, and K. W. Kim, Phys. Rev. B **81**, 121412 (2010).
[20] H. Suzuura and T. Ando, Phys. Rev. B **65**, 235412 (2002).
[21] M.-Q. Long, L. Tang, D. Wang, L. Wang, and Z. Shuai, J. Am. Chem. Soc. **131**, 17728 (2009).
[22] S. Jin, M. V. Fischetti, and T. Tang, J. Appl. Phys. **102**, 083715 (2007).
[23] V. Perebeinos, J. Tersoff, and P. Avouris, Nano Lett. **6**, 205 (2006).
[24] V. Perebeinos, J. Tersoff, and P. Avouris, Phys. Rev. Lett. **94**, 086802 (2005).
[25] V. Perebeinos, S. V. Rotkin, A. G. Petrov, and P. Avouris, Nano Lett. **9**, 312 (2009).